Anal. Chem. **2004,** *76,* 1811−1816

Accelerated Articles

Acquisition of Mid-Infrared Spectra from Nonrepeatable Events with Sub-100-μs Temporal Resolution Using Planar Array Infrared Spectroscopy

Christopher M. Snively,*,†,‡ Christian Pellerin,† John F. Rabolt,† and D. Bruce Chase§

Department of Materials Science and Engineering and Department of Chemical Engineering, University of Delaware, Newark, Delaware 19716, and DuPont Experimental Station, DuPont Inc., Wilmington, Delaware 19880

A novel method is presented that is capable of collecting time-resolved vibrational spectroscopic information with sub-100-μs temporal resolution. Unlike previous step scan FT-IR approaches, the phenomena under study do not necessarily need to be repeatable. The methodology described herein is based on the planar array infrared (PA-IR) technique, which utilizes a spectrograph for wavelength dispersion and a mid-infrared focal plane array (FPA) detector for simultaneous detection of multiple wavelengths. Unlike previous PA-IR approaches, a rolling mode FPA is employed. This unique data readout mode, where data are read out of the array two rows at a time, is exploited to generate increased temporal resolution. The capabilities of this technique are demonstrated using the example of the electric field-induced Freedericksz transition of a nematic liquid crystal. It is shown that the orientational dynamics of a single transition can be tracked over a spectral range of 154 cm^{-1} with a temporal resolution of 99.17 μs while requiring a total experimental time of less than 1 s.

A myriad of chemical and physical phenomena occur with characteristic times on the order of nanoseconds to milliseconds, including photochemistry and photophysics of biological[1−3] and chemical[4−6] systems, polymer dynamics,[7,8] and liquid crystal electrooptical behavior.[9−11] The acquisition of time-resolved spectroscopic information from these systems is beneficial in the elucidation of the inherent chemical or physical mechanism behind these processes. The acquisition of time-resolved vibrational spectroscopic information is of particular interest because a wealth of chemical and physical information can be obtained from a wide variety of complex chemical systems.

A variety of approaches have been developed to meet the need of acquiring time-resolved infrared spectra. The most common approach in recent years has been step scan time-resolved FT-IR spectroscopy, which underwent a renaissance in the late 1980s.[12,13] The step scan technique has the advantage of decoupling the temporal response of the system under study from the modula-

* To whom correspondence should be addressed: snively@che.udel.edu.
† Department of Materials Science and Engineering, University of Delaware.
‡ Department of Chemical Engineering, University of Delaware.
§ DuPont Inc.

(1) Hein, M.; Wegener, A. A.; Engelhard, M.; Siebert, F. *Biophys. J.* **2003**, *84*, 1208−1217.
(2) Hessling, B.; Herbst, J.; Rammelsberg, R.; Gerwert, K. *Biophys. J.* **1997**, *73*, 2071−2080.
(3) Koutsoupakis, C.; Soulimane, T.; Varotsis, C. *J. Am. Chem. Soc.* **2003**, *125*, 14728−14732.
(4) Smith, G. D.; Hutson, M. S.; Lu, Y.; Tierney, M. T.; Grinstaff, M. W.; Palmer, R. A. *Appl. Spectrosc.* **2001**, *55*, 637−642.
(5) Shagal, A.; Schultz, R. H. *Organometallics* **2002**, *21*, 5657−5665.
(6) Kuimova, M. K.; Alsindi, W. Z.; Dyer, J.; Grills, D. C.; Jina, O. S.; Matousek, P.; Parker, A. W.; Portius, P.; Sun, X. Z.; Towrie, M.; Wilson, C.; Yang, J. X.; George, M. W. *Dalton Trans.* **2003**, 3996−4006.
(7) Wang, H. C.; Aubuchon, S. R.; Thompson, D. G.; Osborn, J. C.; Marsh, A. L.; Nichols, W. R.; Schoonover, J. R.; Palmer, R. A. *Macromolecules* **2002**, *35*, 8794−8801.
(8) Marcott, C.; Story, G. M.; Dowrey, A. E.; Reeder, R. C.; Noda, I. *Mikrochim. Acta* **1997**, 157−163.
(9) Prigann, J.; Shilov, S. V.; Skupin, H.; Kremer, F.; Heppke, G.; Rauch, S. *Mol. Cryst. Liq. Cryst.* **2001**, *359*, 699−706.
(10) Nakano, T.; Yokoyama, T.; Toriumi, H. *Appl. Spectrosc.* **1993**, *47*, 1354−1366.
(11) Jordanov, B.; Okretic, S.; Siesler, H. W. *Appl. Spectrosc.* **1997**, *51*, 447−449.
(12) Palmer, R. A.; Manning, C. J.; Rzepiela, J. A.; Widder, J. M.; Chao, J. L. *Appl. Spectrosc.* **1989**, *43*, 193−195.
(13) Manning, C. J.; Palmer, R. A.; Chao, J. L. *Rev. Sci. Instrum.* **1991**, *62*, 1219−1229.

10.1021/ac0499118 CCC: $27.50
Published on Web 02/28/2004

tions induced by the interferometer, thereby allowing the study of processes with characteristic times ranging from seconds to picoseconds using the same technique. Additionally, the flexibility of this Fourier transform technique allows complete spectral coverage from UV to the far-infrared and has even been extended to an imaging modality.[14] The distinct disadvantage of this approach to time-resolved spectroscopy is that the phenomenon under study must be repeated many times, typically on the order of thousands, for the acquisition of a single experimental data set. In order for this approach to provide an accurate account of the phenomenon under study, the sample response must be identical for each of these repetitions. Any sample deterioration occurring during the experiment will change the dynamic response, thereby altering the final results of the experiment. The assumption must often be made that these types of changes do not occur, since it cannot be experimentally verified. This also places limitations on the extent to which the sample can be perturbed during each cycle. For example, in the case of polymer deformation studies, the strain must be kept to a low enough level to remain within the elastic deformation regime.

Some commercial FT-IR spectrometers are capable of acquiring spectra at a fast rate simply by increasing the scanning speed of the interferometer. While this approach requires no special equipment, the reduction in duty cycle imposed by the time required for slowing the mirror and reversing its direction limits this approach to the acquisition of ~100 spectra/s. Recently, advances have been made that allow FT-IR spectra to be acquired much faster.[15−17] By utilizing a specially designed interferometer with a rotating mirror arrangement, spectra can be continuously collected with a temporal resolution of ~5 ms. While this approach shows much promise, it is currently limited in temporal resolution due to engineering limitations that cannot be solved using currently available construction materials and the lack of sufficiently fast analog-to-digital converters.[15]

The use of dispersive instrumentation has been a viable approach for the acquisition of time-resolved spectral information. By using a monochromator tuned to a narrow band of wavelengths and a sufficiently fast single-element detector, time-resolved spectral information can be obtained from a single spectral band with sub-microsecond time resolution.[18,19] This approach is limited to single-wavelength monitoring. A different approach, which combines the Fourier transform and dispersive techniques, has been applied to the acquisition of spectral information from the UV to mid-infrared spectral regions.[20−24] While this instrumental configuration offers increased throughput and no moving parts, it is limited to relatively low resolution applications.

Another dispersive approach involves the combination of a multielement detector with a monochromator in a spectrograph arrangement, such that multiple wavelengths can be acquired simultaneously. This approach has been revived recently[25−27] in the form of planar array infrared (PA-IR) spectroscopy, aided by the increased availability of near- and mid-infrared sensitive focal plane array (FPA) detectors. A similar approach has also been recently applied to the acquisition of infrared spectra with picosecond temporal resolution.[28,29]

PA-IR spectroscopy has been used primarily as a technique for the acquisition of spectral information from static samples but has recently been extended to dynamic phenomena.[27] In these studies, data were collected using a "snapshot mode" FPA, which acquires data simultaneously from all pixels in the array over the same integration time. Since multiple wavelengths are collected simultaneously within each frame of data, time resolution can be achieved by simply collecting multiple frames, with each frame containing data from a single time resolution element. This approach has the advantage of being able to acquire infrared spectral information from events without the necessity of repeating them. The incorporation of a snapshot mode FPA into the experimental setup has the additional advantage of allowing more complicated types of experiments to be performed. For example, real-time background subtraction or real-time dichroic ratio determination can be realized by an appropriate arrangement of the optical setup. This approach possesses one distinct disadvantage, however, in that the data collection duty cycle is extremely low. For example, with a frame rate of 114.89 Hz and an integration time of 80 μs, the duty cycle is only 0.9%; thus, only a fraction of the experimental time is spent on acquisition of data. Thus, even though data are acquired over 80 μs, the temporal resolution of the technique is limited by the frame rate to 8.7 ms.

In this study, a "rolling mode" FPA is employed for data acquisition. In this acquisition scheme, adjacent pairs of rows are constantly read out of the array, such that the duty cycle is 100%. A consequence of rolling mode acquisition is that the integration time is not adjustable but is fixed as a function of the frame rate. For example, with the 64 × 64 pixel FPA used in this study, the integration time is fixed at $^1/_{32}$ of the frame time. This inflexibility can be disadvantageous for some experiments but is used to advantage in this study as a method of generating temporal resolution. The data collected from each pair of rows during an experiment carry information from a single temporal resolution element. Unlike the above-described case of a snapshot mode FPA, the data from a single frame carry information from 32 different temporal resolution elements. With this approach, the maximum achievable time resolution is determined by the integration time. For the rolling mode FPA used in this study, the maximum useable frame rate[30] is 315.13 Hz, with a corresponding integration

(14) Bhargava, R.; Levin, I. W. *Appl. Spectrosc.* **2003**, *57*, 357−366.
(15) Yang, H. E.; Griffiths, P. R.; Manning, C. J. *Appl. Spectrosc.* **2002**, *56*, 1281−1288.
(16) Griffiths, P. R.; Hirsche, B. L.; Manning, C. J. *Vib. Spectrosc.* **1999**, *19*, 165−176.
(17) Pellerin, C.; Prud'homme, R. E.; Pezolet, M.; Weinstock, B. A.; Griffiths, P. R. *Macromolecules* **2003**, *36*, 4838−4843.
(18) Urano, T. I.; Hamaguchi, H. O. *Appl. Spectrosc.* **1993**, *47*, 2108−2113.
(19) Urano, T. I.; Machida, S.; Sano, K. *Chem. Phys. Lett.* **1995**, *242*, 471−477.
(20) Okamoto, T.; Kawata, S.; Minami, S. *Appl. Opt.* **1984**, *23*, 269−273.
(21) Sweedler, J. V.; Denton, M. B. *Appl. Spectrosc.* **1989**, *43*, 1378−1384.
(22) Hashimoto, M.; Kawata, S. *Appl. Opt.* **1992**, *31*, 6096−6101.
(23) Ebizuka, N.; Wakaki, M.; Kobayashi, Y.; Sato, S. *Appl. Opt.* **1995**, *34*, 7899−7906.
(24) Hashimoto, M.; Hamaguchi, H. O. *Appl. Spectrosc.* **1996**, *50*, 1030−1033.
(25) Elmore, D. L.; Tsao, M. W.; Frisk, S.; Chase, D. B.; Rabolt, J. F. *Appl. Spectrosc.* **2002**, *56*, 145−149.
(26) Elmore, D. L.; Leverette, C. L.; Chase, D. B.; Kalambur, A. T.; Liu, Y. J.; Rabolt, J. F. *Langmuir* **2003**, *19*, 3519−3524.
(27) Pellerin, C.; Snively, C. M.; Chase, D. B.; Rabolt, J. F. *Appl. Spectrosc.*, in press.
(28) Towrie, M.; Grills, D. C.; Dyer, J.; Weinstein, J. A.; Matousek, P.; Barton, R.; Bailey, P. D.; Subramaniam, N.; Kwok, W. M.; Ma, C. S.; Phillips, D.; Parker, A. W.; George, M. W. *Appl. Spectrosc.* **2003**, *57*, 367−380.
(29) Hamm, P.; Wiemann, S.; Zurek, M.; Zinth, W. *Opt. Lett.* **1994**, *19*, 1642−1644.

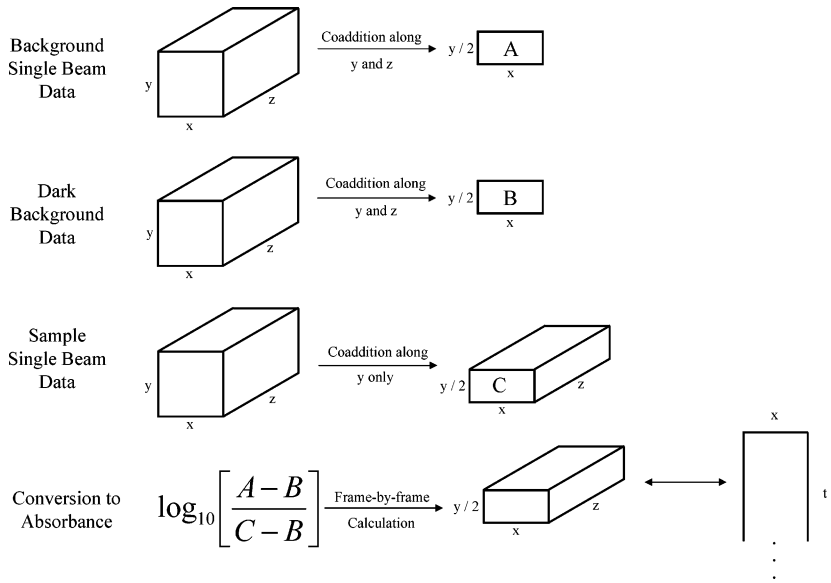

Figure 1. Schematic of data processing steps used to arrive at time-resolved absorbance spectra from the sample, background, and dark background data files.

time of 99.17 μs. In order for the same time resolution to be achieved with a snapshot mode FPA, the frame rate would need to be over 10 kHz. While such technology exists, availability and cost limitations preclude this from being a viable experimental approach to routine time-resolved spectroscopy, and the advantage of implementing a rolling mode FPA into the PA-IR setup becomes apparent. Time-resolved spectral information can be acquired from events that are not necessarily reproducible with a higher temporal resolution than can be achieved using a snapshot mode FPA.

The use of a rolling mode FPA has several negative effects that must also be considered. The aforementioned more complex experiments that can be performed with a snapshot mode FPA cannot be performed with a rolling mode FPA, since data from different rows in the array are collected at different times. Additionally, only two spectra can be averaged for each temporal resolution element. This may prove to be a limitation for experiments that have low throughput or those in which small changes in absorbance are present.

EXPERIMENTAL SECTION

The experimental setup used in this study is similar to that described in recent publications.[25−27] Briefly, the setup is composed of a Czerny−Turner spectrograph equipped with an air-cooled globar source, a 400-μm entrance slit, a 5-μm long-pass order-sorting filter, and a 64 × 64 pixel mercury cadmium telluride FPA detector (Santa Barbara Focalplane, Goleta, CA) equipped with a multielement lens (Janos Technology Inc., Townsend, VT). The grating employed in this study had 150 grooves/mm and was blazed at a wavelength of 6.0 μm and a blaze angle of 26.7°. All experiments were performed without the aid of a purged environment, under laboratory conditions of approximately 22 °C and 25% relative humidity. Data were acquired using a frame rate of 315.13 Hz, with a corresponding integration time of 99.17 μs.

Data collection consisted of the acquisition of a background (single-beam) data set and a dark background data set before the sample data were acquired. Typically, to increase the signal-to-noise ratio (SNR) of the final processed data, multiple frames were collected and averaged for both the background and dark background data sets. The steps involved in the data processing are shown schematically in Figure 1.

First, the background and dark background data sets undergo two types of averaging: each pair of rows within each frame is averaged, along the *y*-dimension, to reduce the size of each frame to 64 × 32; these reduced frames are subsequently averaged, along the *z*-dimension, such that the final data set size is 64 × 32. Since the sample data set contains time-resolved information both along the *y*-axis within each frame and along the *z*-axis among frames, coaddition was only applied along the *y*-axis, to arrive at a final sample data set size of 64 × 32 × *N*, where *N* is the number of frames collected during the experiment. After the dark backgrounds were subtracted frame by frame from the sample and background data sets, a base-10 logarithm operation was used to convert the data into a series of time-resolved absorbance spectra.

Custom software was written in C++ and implemented on a standard desktop PC computer to carry out all of the above processing steps. Additional processing was performed in GRAMS (ThermoGalactic, Salem, NH), where the integration routine was employed to extract the baselined peak height as a function of time. This was necessary due to the spectral shift caused by the particular optical setup employed in this study (vide infra). Nonlinear curve fitting was performed in Origin (OriginLab Corp., Northampton, MA).

As an example, the electric field-induced Freedericksz transition of a low molecular weight liquid crystal was chosen. 4-*n*-Pentyl-4′-cyanobiphenyl (5CB) was sandwiched between 50 × 20 × 2 mm Ge plates. Homogeneous alignment of the liquid crystal was established by solvent casting a thin film of poly(vinyl alcohol) onto the substrates, followed by unidirectional rubbing with a cotton swab. This sample preparation method causes the liquid crystal molecules to align with their molecular long axes along the rubbing direction of the substrate, to minimize the elastic

(30) The maximum frame rate available with our current setup was 420 Hz, but the presence of excessive amounts of noise at this frame rate precluded its use.

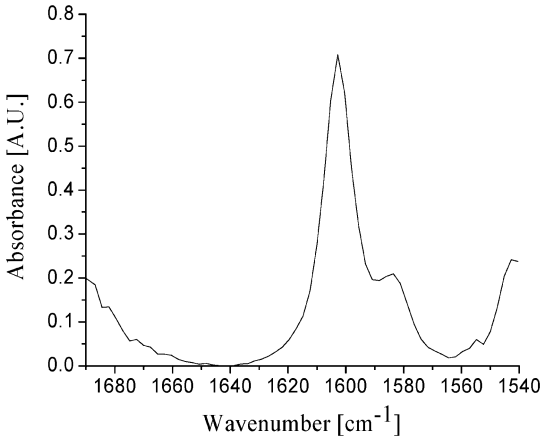

Figure 2. Example spectrum of polystyrene showing the data quality that can be obtained. This spectrum was extracted from the middle row of the image shown in Figure 3.

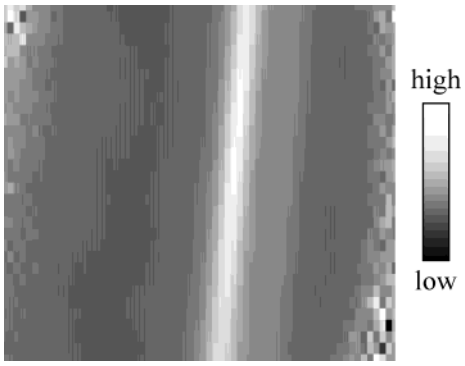

Figure 3. Image from a single frame of absorbance data acquired from a polystyrene film. The speckled patterns on the sides of the image are caused by increased noise due to low signal in these regions.

free energy of the system.[31] The thickness of the sample was maintained through the use of 15-μm glass rod spacers. Electrooptical switching was induced by the application of a 100-ms pulse of a 10-V_{p-p}, 1-kHz sinusoidal electric field to wires that were attached to the edges of the Ge plates with silver paint.

For comparison purposes, FT-IR spectra were acquired from 5CB using a FT-IR spectrometer (Bruker Equinox 55) set to various spectral resolutions. These spectra were processed with no zero filling and triangular apodization in order to most directly compare them with the PA-IR spectra. The wavelength scale for the PA-IR data was calibrated by comparing an absorbance spectrum acquired from a 38-μm-thick polystyrene film with that acquired using the FT-IR spectrometer.

RESULTS AND DISCUSSION

By comparison with the FT-IR spectra, the spectral range of the time-resolved PA-IR data was found to be 154 cm^{-1}, with a spectral resolution of ~8 cm^{-1}. These are different from previously reported PA-IR results because the higher groove density of the grating employed in this study (150/mm as compared with 50/mm) improves the spectral resolution. However, due to the larger pixel pitch (61 μm) and smaller overall size of the FPA (4 mm), the total spectral range is smaller. It should be noted that the spectral resolution is not as high as it could be. For 64 pixels spanning a 154-cm^{-1} range, the resolution could theoretically be as high as 2.4 cm^{-1} but is not realized in this case because a wider than necessary slit width was used to provide increased throughput. This was necessary due to the thickness of the Ge plates used for the sample. An example of the data quality that can be obtained using this technique is shown in Figure 2, which shows a spectrum extracted from the polystyrene calibration data set. This spectrum was generated by coadding two rows of sample data and 128 frames of background data, which provides an absorbance SNR of almost 200 for the 1601-cm^{-1} band. The rising baseline at the edges of the spectrum is caused by nonuniform light intensity at the edges of the image. The stability of this configuration with time is comparable to that using a snapshot mode FPA.[27]

Two optical effects should be considered before attempting to interpret the time-resolved data collected using this technique. The first is the presence of field curvature caused by the utilization of spherical mirrors in an off-axis arrangement. While this curvature can be minimized by proper adjustment of the optical setup, it cannot be completely eliminated without employing different optics or a curved slit.[32] In the optical setup employed here, a relatively small shift of only four pixels from the top to the bottom of the image is present and can be seen upon inspection of a single image frame extracted from the polystyrene calibration data set, as shown in Figure 3. The light vertical streaks near the center of the image are from the 1601- and 1583-cm^{-1} bands.

The second effect that should be considered is the interplay between the dispersion of the spectrograph and the pixel pitch of the array detector. These two parameters must be chosen such that the resulting spectral resolution is high enough to properly resolve the spectral bands of interest. If this condition is not met, peaks that have a natural line width narrower than the resolution will appear to be clipped. Additionally, this clipping will vary as a function of position along the image, due to the above-mentioned curvature, leading to wide row-by-row variations of the peak shape and intensity. The FPA used in this study possesses a pixel pitch of 61 μm, which is substantially larger than the 40-μm pixel pitch of the array used in previous studies.[27] Preliminary spectra acquired using a grating with 50 grooves/mm exhibited peak clipping. This lead to spectral artifacts that masked the time-resolved spectral changes and demonstrated the necessity of using a grating with 150 grooves/mm. This effect would not be a concern if the SNR and frame rate of the FPA were sufficient to use only one row of data per frame. This, however, would only be possible with very fast and sensitive FPAs.

Using peak area instead of peak height as a quantitative measure can eliminate the effect of field curvature, but only under the fortuitous circumstance of a flat baseline and constant noise level around the band of interest. Additionally, if peak overlap exists, this approach would not work without more advanced processing, such as peak fitting. Alternatively, the baselined peak height can be used, if proper care is taken to ensure that the absorbance value at the actual peak maximum is used, since the

(31) Berreman, D. W. *Phys. Rev. Lett.* **1972**, *28*, 1683−1686.

(32) Zhao, J. *Appl. Spectrosc.* **2003**, *57*, 1368−1375.

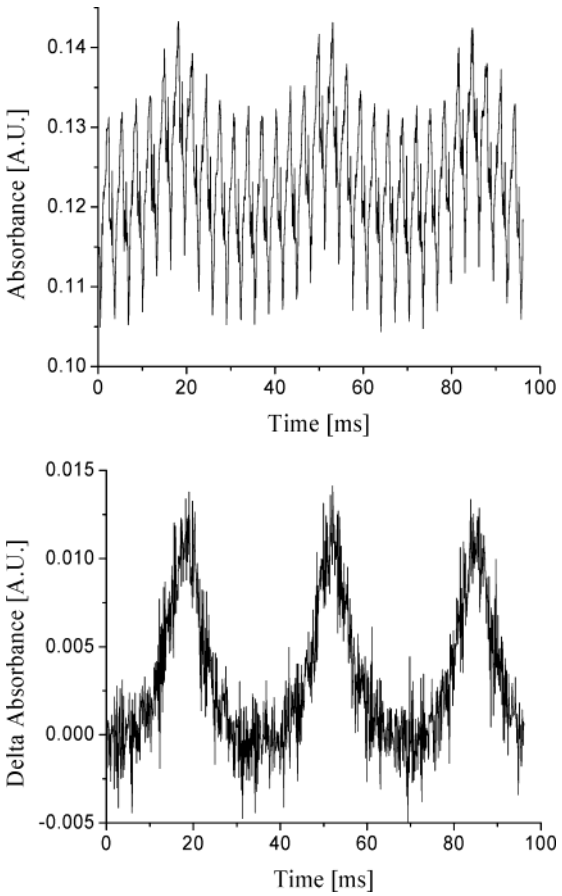

Figure 4. Traces generated by plotting the 1606-cm^{-1} C═C stretching mode of 5CB as a function of time during the application of a 15-Hz, 10-V_{p-p} electric field. (top) Data processed with the steps shown in Figure 1. (bottom) Data from the top trace processed with an additional subtractive normalization (see text).

peak maximum shifts as a function of position along the image. This can be conveniently implemented in commercially available software and was the approach used in this paper. Even with this correction, however, some row-to-row variations remain in the data and can be sufficiently strong enough to obscure the phenomena being observed. The trace on the top of Figure 4 shows the result of plotting the baselined peak height (keeping the spectral shift in mind) as a function of time for a 5CB sample that was subjected to a 15-Hz, 10-V_{p-p} sine wave. While some of the expected oscillatory behavior is apparent in this figure, it is overshadowed by another oscillatory component of much higher frequency caused by a periodic variation in response as a function of position within the image. This variation in response is caused by the above-mentioned nonideal optical setup. One final processing step was employed to remove this component. An entire frame (64 × 32) of data from a time period before the event of interest was subtracted from the entire data set in a frame-by-frame manner, such that the data were converted to a delta absorbance scale. The result of this operation is presented in the bottom trace of Figure 4, which shows that the previously observed periodic variation in intensity has been effectively damped out, leaving behind only the contribution from the applied electric field.

Time-resolved spectral data acquired during the electrooptical switching of 5CB are shown in Figures 5 and 6. These traces were generated by plotting the fully corrected absorbance intensity of

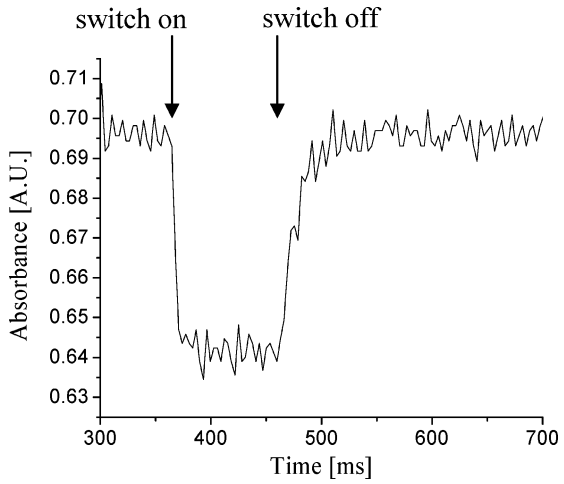

Figure 5. Low temporal resolution (3.17 ms) trace of the electrooptical switching of 5CB using a 100-ms electric field pulse, generated by plotting the absorbance value from one spectrum per frame of data.

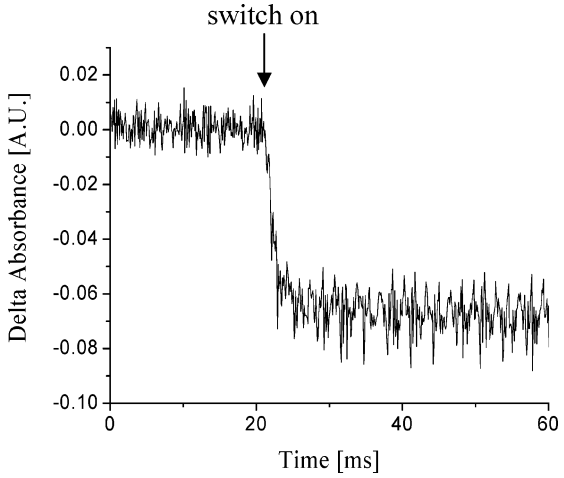

Figure 6. Switch-on region of the same data set used to generate Figure 5, with the data plotted at the maximum temporal resolution of 99.17 μs. These data were plotted using the subtractive normalization illustrated in Figure 4.

the 1606-cm^{-1} phenyl C═C stretching band as a function of time. When an electric field is applied to the sample, the orientation of the liquid crystal molecules changes such that their molecular long axes align along the direction of the field. If the transition dipole moment of the band of interest is directed along the direction of the molecular long axis, as is the case for the phenyl C═C stretching band, the application of this field manifests itself through a decrease in the absorbance intensity of the band. Upon removal of the field, the liquid crystal molecules return to their original homogeneous alignment, and the absorbance of the band increases to its original value before the application of the electric field. Figure 5 is a low time resolution (3.17 ms) trace, generated by extracting the absorbance values from only a single row of each frame in the data set. This case reduces to that of using a single pair of rows from a snapshot mode FPA. Figure 6 is a high time resolution trace generated by plotting the same data set that was used to generate Figure 5, except at the maximum time resolution of 99.17 μs. The improvement in temporal resolution is apparent when the number of data points in the transient region immediately after the field was applied is considered. In the low

Table 1. Time Constants Obtained from the Switch-On and Switch-Off Portions of the Response Curves for 5CB

no. of switches	switch-on time constant (ms)	error (±)	switch-off time constant (ms)	error (±)
1	1.40	0.10	19.5	1.5
2	1.53	0.14	17.6	1.5
3	1.49	0.11	18.8	1.5
4	1.55	0.11	14.6	1.6
5	1.72	0.13	19.4	1.6
6	1.76	0.12	13.3	1.4
7	1.45	0.11	20.5	1.8
8	1.47	0.11	17.2	1.7
9	2.03	0.11	15.0	1.3
10	1.35	0.10	16.8	1.8
100	1.49	0.09	13.9	0.9
300	1.33	0.11	20.3	1.5

time resolution trace, there are only three data points in the transient region, while there are almost 100 data points in this region of the high time resolution trace.

The portion of the curve in Figure 5 from times after the electric field pulse was removed (switch-off) was fitted with a single-exponential function. The portion of the curve in Figure 6 immediately following the application of the field (switch-on) was fitted to a single-exponential decay function. The time constants from both the switch-on and switch-off portions of the curve for the first 10 switches were determined and are shown in Table 1. The sample was additionally switched several hundred times, and the time constants from the 100th and 300th switches are also shown in the table. From these data, it can be seen that the electrooptical behavior does not significantly change as the sample is switched. The importance of this table lies in the fact that this behavior was explicitly determined and was not assumed, which is the approach that must be taken in time-resolved step scan FT-IR experiments.

An additional feature of this approach is that a direct tradeoff can be made between time resolution and SNR. If a higher SNR is desired, the number of subsequent rows that are averaged together can be increased. This simultaneously decreases the temporal resolution, in direct proportion to the number of pairs of subsequent rows that are averaged. This can be implemented simply through software and will provide the standard square root increase in signal-to-noise ratio at the expense of temporal resolution. Finally, in the case of repeatable events, it is possible to average the data acquired from several cycles in order to achieve the desired SNR. This would preserve the higher temporal resolution of the technique, while allowing the experiment to be performed much faster than with a step scan FT-IR approach.

CONCLUSIONS

We have shown that mid-infrared spectra can be acquired from nonreproducible events with sub-100-μs time resolution. This approach has potential for application to the study of a wide range of irreversible chemical and physical changes. This technique is flexible and can be extended to the collection of spectra with a broader spectral range or higher spectral resolution than that demonstrated here by simply employing a different grating or FPA. As faster FPAs become available, the time resolution of this technique will also increase. While future advances in FPA technology are pointing toward snapshot mode data acquisition as the norm, applications such as this one may warrant further exploration into the future development of rolling mode arrays.

ACKNOWLEDGMENT

The authors thank Prof. Jochen Lauterbach (Chemical Engineering, University of Delaware) for the gracious loan of the focal plane array detector used for the collection of data in this study and the National Science Foundation (CHE-0346454-ACT and NSF-DMR-0315461) for their generous support during the course of this work.

Received for review January 14, 2004. Accepted February 17, 2004.

AC0499118